OPEN ACCESS
IOP Publishing
Journal of Physics A: Mathematical and Theoretical
J. Phys. A: Math. Theor. **56** (2023) 485206 (24pp) https://doi.org/10.1088/1751-8121/ad04a3

Quantum curl forces

M V Berry[1,*] **and Pragya Shukla**[2]

[1] H H Wills Physics Laboratory, Tyndall Avenue, Bristol BS8 1TL, United Kingdom
[2] Department of Physics, Indian Institute of Technology, Kharagpur 721302, India

E-mail: asymptotico@bristol.ac.uk

Received 9 May 2023; revised 14 September 2023
Accepted for publication 18 October 2023
Published 13 November 2023

Abstract

Classical nonhamiltonian dynamics, driven by external 'curl forces' (which are not the gradient of a potential) is extended to the quantum domain. This is a generalisation of the two-stage Madelung procedure for the quantum Hamiltonian case: (i) considering not individual trajectories but families of them, characterised by their velocity and density fields (both functions of position and in general time); and (ii) adding the gradient of the quantum potential to the external curl force. Curl forces require the velocity field to have nonzero vorticity, so there is no underlying singlevalued wavefunction. Two explicit examples are presented. A possible experiment would be the motion of small particles with complex polarisability, influenced by forces from optical fields.

Keywords: Madelung, streamlines, Bohmian, phase, nonhamiltonian

(Some figures may appear in colour only in the online journal)

1. Introduction

Newtonian mechanics is more general than Hamiltonian or Lagrangian mechanics. An example is the dynamics of particles driven by 'curl forces' [1]: forces $\boldsymbol{F} = \boldsymbol{F}(\boldsymbol{r})$, depending on position $\boldsymbol{r}$ but not velocity $\boldsymbol{u}$, which are not the gradient of a potential. In the familiar case where there is a potential V, then $\boldsymbol{F} = -\nabla V$ and $\nabla \times \boldsymbol{F} = 0$. For 'curl forces' this is not the case; the classical dynamics is

$$d_t \boldsymbol{r} = d_t \boldsymbol{u} = \boldsymbol{F},\ \nabla \times \boldsymbol{F} \neq 0\ . \tag{1.1}$$

* Author to whom any correspondence should be addressed.

Curl forces contrast with forces derivable from a potential in several ways [1]. Although nonconservative, motion is nondissipative: volume is conserved in the state space $\boldsymbol{r},\boldsymbol{u}$; therefore there are no attractors. Noether's theorem does not apply: the link between symmetries and conservation laws is broken. And there can be dynamical evolutions with no conserved quantity, even though $\boldsymbol{F}$ is independent of time: for N-dimensional configuration space $\boldsymbol{r}$, trajectories can explore a $2N$-dimensional region in $\boldsymbol{r},\boldsymbol{u}$ space [2].

Curl forces do not occur in fundamental classical physics, where forces are associated with potentials. But they are fundamental dynamical mathematics, in the sense that Newton's equation (1.1) is more general than the special case for potential forces. To avoid confusion, we emphasise that the classical curl forces we consider are velocity-independent; as explained earlier [1], this excludes magnetic forces, where $\boldsymbol{F}$ depends on $\boldsymbol{u}$ as well as $\boldsymbol{r}$ and there is a familiar Hamiltonian description. Curl forces appear as emergent forces: approximate descriptions, in engineering [3–5], and as a class of forces exerted by optical fields on small dielectric particles with complex polarisability [6].

Here we explore the natural question: can the concept of curl forces be extended to quantum mechanics? At first thought, the answer is no, because in its standard formulation quantum physics is fundamentally Hamiltonian. But we will propose a natural generalisation of quantum mechanics that does incorporate curl forces. This is based on the Madelung picture of quantum mechanics [7] described later, developed from ideas of de Broglie [8], and formally equivalent to 'Bohmian mechanics' [9, 10]. Extending Madelung mechanics to include velocity fields with vorticity has been considered before [11–14]; our emphasis here is the connection with curl forces.

The paper is structured as follows. Section 2 contains the quantum curl force formalism, emphasising its differences from familiar quantum mechanics. Section 3 describes a quantum curl force where $\nabla\times\boldsymbol{F}$ is nonzero only at the origin, and suitably adapted techniques from conventional quantum mechanics can be applied if the origin is excluded. Section 4 describes a quantum velocity field with streamlines on cylinders. The concluding section 5 includes a suggestion for possible experiments involving quantum curl forces.

Appendix 1 shows that Madelung quantum mechanics, and therefore our curl force generalisation, also apply where the kinetic energy is an anisotropic function of velocity. Appendix 2 supplies two checks on the calculations in section 3. Appendix 3 elaborates and generalises an issue arising in section 3, concerning angle variables in the plane and 'unwrapped' on a helicoid. Appendix 4 explores the continuity relation between the flow velocity and its density for steady flows.

We emphasise that we are not proposing quantum curl force dynamics as a fundamental alternative to well-established standard quantum physics. Rather, we regard it as a formalism worth exploring, which could have application as a higher-level approximate ('effective', or 'emergent') theory, as for classical curl forces [6]. We are also agnostic on questions of interpretation, for example concerning the physical meaning of the trajectories in conventional quantum mechanics or our generalisation to curl forces; we employ Madelung's formulation, and do not discuss the philosophical aspects commonly considered in 'Bohmian mechanics' [15]. Nor will we be concerned with the mathematical subtleties of the precise relation between the Madelung and Schrödinger pictures, well explored elsewhere [16–18].

2. Formulation

We will simplify writing by indicating the arguments of functions only where necessary to avoid confusion, and will use units where the particle mass, and also $\hbar$ (except in section 3), are unity.

We need to review the Madelung (hydrodynamic) picture [7, 15] of familiar quantum mechanics. Waves satisfying the Schrödinger equation are written in the polar form

$$\psi = \psi(\boldsymbol{r},t) = \sqrt{\rho}\exp(i\chi), \tag{2.1}$$

with ρ regarded as a density at position $\boldsymbol{r}$ and time t, and the phase gradient

$$\boldsymbol{u} = \nabla\chi \tag{2.2}$$

as a quantum flow velocity. There are two fundamental differences from classical Hamiltonian particle dynamics. First, the flow describes a family of trajectories: $\boldsymbol{u}$ is a flow field, depending on $\boldsymbol{r}$ and t, not the velocity of an isolated single trajectory. Second, the dynamics is supplemented by the force from a quantum potential. Thus

$$\begin{gathered} d_t\boldsymbol{u} = \partial_t\boldsymbol{u} + \boldsymbol{u}\cdot\nabla\boldsymbol{u} = \boldsymbol{F} - \nabla V_Q, \\ \text{where } \boldsymbol{F} = -\nabla V \text{ and } V_Q = -\frac{\nabla^2\sqrt{\rho}}{2\sqrt{\rho}}. \end{gathered} \tag{2.3}$$

Introducing V_Q is fundamental because it incorporates nonlocality (holism) into the Madelung formulation (trajectories in the family represented by the velocity field $\boldsymbol{u}(\boldsymbol{r})$ are connected by the underlying Schrödinger equation, in contrast with Newtonian trajectories, where the velocity can be specified separately at each point). Temporarily reinstating physical units, $V_Q = \hbar^2\left(\nabla^2\sqrt{\rho}\right)/\left(2m\sqrt{\rho}\right)$, i.e. proportional to $\hbar^2$. Recently, there has been a revival of interest in the quantum potential, with applications to thermodynamics and information theory [19, 20], superoscillations [21, 22], and trajectories in optical beams [23].

The flow $\boldsymbol{u}$ and density ρ are connected by the continuity equation

$$\nabla\cdot(\rho\boldsymbol{u}) = -\partial_t\rho \ . \tag{2.4}$$

The fact that $\boldsymbol{u}$ is a phase gradient implies that the flow is irrotational, i.e. the vorticity $\boldsymbol{\omega}$ vanishes:

$$\omega \equiv \nabla\times\boldsymbol{u} = 0, \tag{2.5}$$

except at zero lines of ψ, around which, to ensure that ψ is singlevalued [11, 16],

$$\oint \boldsymbol{u}\cdot d\boldsymbol{r} = 2n\pi\,. \tag{2.6}$$

This completes the reprise of the Madelung formalism.

Our proposed quantum curl force generalisation retains the picture of a flow field $\rho, \boldsymbol{u}$ and the continuity equation (2.4), which for steady flows is explored further in appendix 4. We also retain (2.3), with the fundamental difference that now $\boldsymbol{F}$ can be a curl force as in (1.1), i.e. $\boldsymbol{F} \neq -\nabla V$. We also discard the circulation condition (2.6). This is important: in the Madelung formulation of conventional quantum (and more generally wave) physics: velocity fields associated with singlevalued wavefunctions can possess vorticity in the form of isolated vortex

lines [13, 24–29], but these are constrained by (2.6); by contrast, although the velocity fields we consider here can possess isolated vortex lines (as in section 3), their circulation is not so constrained.

To understand an important implication of quantum curl force dynamics, we use the identity

$$\boldsymbol{u}\cdot\nabla\boldsymbol{u} = -\boldsymbol{u}\times\omega + \frac{1}{2}\nabla u^2. \tag{2.7}$$

Thus the external force that would generate a given flow is

$$\boldsymbol{F} = -\boldsymbol{u}\times\omega + \partial_t\boldsymbol{u} + \nabla\left(\frac{1}{2}u^2 + V_Q\right), \tag{2.8}$$

i.e.

$$\nabla\times\boldsymbol{F} = -\nabla\times(\boldsymbol{u}\times\boldsymbol{\omega}) + \partial_t\omega\,. \tag{2.9}$$

This involves only the velocity $\boldsymbol{u}$ and its vorticity $\boldsymbol{\omega}$, not the density ρ. If $\boldsymbol{\omega}=0$, $\nabla\times\boldsymbol{F}=0$. The important implication is that quantum curl forces cannot generate irrotational flows: for quantum curl forces, (2.5) is violated. This further implies that $\boldsymbol{u}$ is not a phase gradient as in (2.2), so there is no phase and therefore no singlevalued wavefunction satisfying a Schrödinger equation: all that survives is the flow. As in the Madelung picture of standard quantum mechanics, the field $\boldsymbol{u}=\boldsymbol{u}(\boldsymbol{r},t)$ determines 'quantum trajectories' $\boldsymbol{r}(t)$ by

$$d_t\boldsymbol{r}(t) = \boldsymbol{u}(\boldsymbol{r}(t),t). \tag{2.10}$$

For the important class of steady (i.e. time-independent) flows, the underlying particle trajectories are the streamlines of the velocity field $\boldsymbol{u}$, along which particles move with speed $|\boldsymbol{u}|$. In this case, it follows from (2.9) that Beltrami flows [30], in which the vectors $\boldsymbol{u}$ and $\boldsymbol{\omega}$ are parallel, cannot be generated by curl forces.

Quantum curl dynamics can be regarded as the fourth level in a hierarchy:

Level 1. *Classical conservative Newtonian dynamics*. This is represented by the first of equation (1.1) with $\boldsymbol{F}=-\nabla V$, and quantum potential $V_Q=0$.
Level 2. *Classical curl forces*. This is both equations in (1.1), also with $V_Q=0$.
Level 3. *Quantum Madelung dynamics*. This is (2.3), i.e. (1.1) with $\boldsymbol{F}=-\nabla V$ and $V_Q\neq 0$.
Level 4. *Quantum curl dynamics*. This is the new level: (2.3) with $V_Q\neq 0$ and also $\boldsymbol{F}\neq-\nabla V$.

There is a fundamental difference between the quantum trajectories generated by (2.10) and the corresponding classical trajectories. Classical trajectories in the family representing a quantum state can cross in spacetime; in the semiclassical description, such crossings underly quantum interference. But in families of quantum trajectories, including those generated by curl forces, such crossings are avoided, because the velocity $\boldsymbol{u}$ is uniquely defined for each $\boldsymbol{r},t$. Instead of crossing, quantum trajectories typically represent interference by exhibiting undulations. This will be illustrated in section 3. (To avoid confusion, we note that if the velocity field is time-dependent the tracks of the quantum orbits can cross in $\boldsymbol{r}$ space; this simply corresponds to orbits reaching the same point at different times, at which $\boldsymbol{u}$ is different; this too will be illustrated in section 3.)

The undulation phenomenon is ubiquitous in the physics of waves, not restricted to quantum mechanics, and occurring also in quantum curl force dynamics. Undulations were conjectured by Newton [31] in connection with the intensity oscillations associated with optical edge

diffraction [32], with rays described as having '…a motion like that of an eel' [33, 34] (for undulations in 2-slit interference, or waves from two sources, see [15], figure 3 of [32], and section 2 of [12]). In modern terminology, these different interpretations of interference—semiclassical superposition, and undulations of quantum trajectories—can be expressed in standard wave physics as follows: phase is a nonlinear function of its wavefunction, so the phase gradient of a superposition is different from the superposition of phase gradients [32].)

A cautionary remark. The first equality in (2.3), combined with (2.7), can be written

$$d_t \boldsymbol{u} = \boldsymbol{E} + \boldsymbol{u} \times \boldsymbol{B}, \tag{2.11}$$

involving two fields $\boldsymbol{E}$ and $\boldsymbol{B}$ and their potentials, connected by the vector field $\boldsymbol{u}$:

$$\boldsymbol{B} = \nabla \times \boldsymbol{A}, \text{ with } \boldsymbol{A} = -\boldsymbol{u} \text{ and } \boldsymbol{E} = -\partial_t \boldsymbol{A} - \nabla \Phi, \text{ with } \Phi = -\frac{1}{2} u^2 . \tag{2.12}$$

As has been noted [12, 13], this superficially resembles electromagnetism. The analogy is misleading, for several reasons. First, the pair of equations (2.11) and (2.12) constitutes a tautology: it is satisfied for any $\boldsymbol{u}$ and so cannot determine the (classical or quantum) velocity field or its dynamics. To determine $\boldsymbol{u}$, the contribution from $\boldsymbol{F} - \nabla V_Q$ must be included. Second, the fields $\boldsymbol{E}$ and $\boldsymbol{B}$ do not satisfy Maxwell's equations. Third, the seemingly natural Hamiltonian

$$H = \frac{1}{2}(\boldsymbol{p} - \boldsymbol{A})^2 + \Phi \tag{2.13}$$

generates dynamics different from (2.11).

3. Example: azimuthal force with curl nonzero at a single point

3.1. Formulation

This is the two-dimensional force (in plane polar coordinates r, θ)

$$\boldsymbol{F} = \frac{\boldsymbol{e}_\theta}{r}, \tag{3.1}$$

in which here and hereafter $\boldsymbol{e}$ will denote unit vectors. (A coefficient modifying the strength of $\boldsymbol{F}$ can be eliminated by scaling r and t in the Schrödinger equations to follow.) $\boldsymbol{F}$ is a curl force with circular symmetry (i.e. invariant under rotations). The curl is nonzero only at $\boldsymbol{r} = 0$; the circulation around any loop surrounding the origin is constant, so, from Stokes's theorem,

$$\nabla \times \boldsymbol{F} = 2\pi \delta(\boldsymbol{r}) . \tag{3.2}$$

Excluding the origin, $\boldsymbol{F}$ can be written as the minus the gradient of the scalar potential

$$V(\boldsymbol{r}) = -\theta, \tag{3.3}$$

whose domain is the full line $-\infty < \theta < \infty$, i.e. including windings, not the plane angle $0 \leqslant \theta < 2\pi$. For this case, in contrast to general curl forces, there is a Hamiltonian; excluding $\boldsymbol{r} = 0$, this is

$$H_1 = \frac{1}{2}\, \boldsymbol{p} \cdot \boldsymbol{p} - \theta. \tag{3.4}$$

Earlier [1], we considered the classical particle dynamics generated by H_1, and will return to this later. Our main concern here is the quantum dynamics. For this particular curl force, where $\nabla \times \boldsymbol{F}$ is concentrated at a point, there is an underlying Schrödinger equation, namely (for particle mass defined as unity)

$$i\hbar\partial_t\psi = -\frac{1}{2}\hbar^2\nabla^2\psi - \theta\psi\,, \tag{3.5}$$

in which we now write $\hbar$ explicitly. But the Hamiltonian H_1 is not singlevalued in θ, i.e. the potential violates the circular symmetry of the force, reflecting its nonzero curl. The solutions of (3.5) are not plane-periodic but are smooth and singlevalued on the helicoid, with windings specified by the integer $(\theta - \theta\,(\mathrm{mod}\,2\pi))\,/\,(2\pi)$; see appendix 3 for more discussion.

Circular symmetry can be restored by the time-dependent gauge transformation

$$\psi = \exp\left(i\frac{\theta t}{\hbar}\right)\Psi\,, \tag{3.6}$$

where Ψ satisfies

$$\begin{aligned} i\hbar\partial_t\Psi &= H_2\Psi = \frac{1}{2}\,(\boldsymbol{p}-\boldsymbol{A})^2\Psi = \frac{1}{2}\left(-i\hbar\nabla + \frac{te_\theta}{r}\right)^2\Psi \\ &= -\frac{\hbar^2}{2r}\partial_r r\partial_r\Psi - \frac{\hbar^2}{2r^2}\partial_{\theta\theta}\Psi - \frac{i\hbar t}{r^2}\partial_\theta\Psi + \frac{t^2}{2r^2}\Psi\,. \end{aligned} \tag{3.7}$$

Physically, the time-independent curl force Hamiltonian H_1, whose solutions are singlevalued on the helicoid but not the plane, has been replaced by the time-dependent Hamiltonian H_2 (3.7); this is periodic in θ and its solutions are singlevalued on the punctured plane.

The Hamiltonian H_2 represents an intriguing variant of the Aharonov–Bohm effect: it corresponds, as noted earlier [1], to the motion of a charged quantum particle in the presence of a line of magnetic flux whose strength increases linearly with time, located at the origin. The relation between solutions of the 'unwrapped' Hamiltonion H_1 and those of the periodic H_2 is the Poisson sum formula, elaborated and described in a more general context in appendix 3.

With circular symmetry restored and θ eliminated, the Hamiltonian H_2 is separable in r and θ, so Ψ can be written as a superposition of partial waves. Reinstating the variables,

$$\Psi\,(r,\theta,t) = \sum_m c_m \exp(im\theta)\,R\,(r,t+m\hbar)\,, \tag{3.8}$$

where the radial wavefunction satisfies

$$i\hbar\partial_t R\,(r,t) = -\frac{\hbar^2}{2r}\partial_r\,(r\partial_r R\,(r,t)) + \frac{t^2}{2r^2}R\,(r,t)\ . \tag{3.9}$$

In the representation H_1, the angular momentum is

$$\hbar\partial_\theta \arg\psi = m\hbar + t. \tag{3.10}$$

Thus the circulation condition (2.6) is violated. There is no vector potential, so the kinetic and canonical angular momenta are equal. In the representation H_2, $\hbar\partial_\theta \arg\psi = m\hbar$ is the conserved canonical angular momentum, and by adding $-r\boldsymbol{A}\cdot\boldsymbol{e}_\theta = t$ the gauge-invariant kinetic angular momentum (3.10) is regained, and the circulation condition (2.6) restored. The gauge-invariant angular momentum (3.10) is not conserved; as noted earlier in the classical case,

this increases linearly in time, illustrating the non-applicability of Noether's theorem in the presence of the curl force (3.1) which possesses rotational symmetry.

Since the angular quantum number appears only in the combination $t+m\hbar$, we need consider only $m=0$; the amplitudes of the other partial waves in the superposition (3.8) can be obtained simply by time translation.

The gauge transformation (3.6) has replaced the Hamiltonian H_1, whose Schrödinger equation (3.5) is separable in r,t but not r,θ, by the Hamiltonian H_2, whose Schrödinger equation (3.7) is separable in r,θ but not r,t. This is a simplification because the radial equation (3.9) is first-order in t, which can be more easily solved numerically for any initial state $R_0(r)\equiv R(r,0)$.

The quantities of interest in our quantum curl theory are the density ρ and the velocity $\boldsymbol{u}$. For the partial wave m, these are

$$\rho=|R(r,t)|^2,\quad \boldsymbol{u}=\hbar\nabla\arg\psi=\hbar\partial_r\arg R(r,t)\,\boldsymbol{e}_r+\frac{t}{r}\boldsymbol{e}_\theta \tag{3.11}$$

with $t\to t+m\hbar$. The velocity $\boldsymbol{u}$ is not irrotational; its vorticity $\boldsymbol{\omega}$, reflecting its origin in the curl force (3.1), is concentrated at the origin:

$$\boldsymbol{\omega}=2\pi\, t\delta(\boldsymbol{r}) \tag{3.12}$$

(cf. the corresponding formula (3.2) for $\nabla\times\boldsymbol{F}$). Concentrated vorticity (i.e. vortex lines in three-dimensional space) has been studied [13] for the special case where its strength is time-independent, in contrast to (3.12).

3.2. Radial dynamics

To illustrate these results, we invoke separability and consider first the r dynamics, and incorporate θ later. As a convenient normalised initial state, we choose a semiclassically narrow Gaussian at $r=r_0$, approximating $\delta(r-r_0)$. In the position and momentum (=velocity) representation, and with generic constants K,

$$\begin{aligned}R_0(r)&=K\exp\left(-\frac{(r-r_0)^2\Pi^2}{2\hbar^2}\right),\\ \bar{R}_0(v_0)&=K\exp\left(-i\frac{r_0v_0}{\hbar}\right)\exp\left(-\frac{v_0^2}{2\Pi^2}\right).\end{aligned} \tag{3.13}$$

This choice has the advantage that the velocity intensity distribution does not involve $\hbar$, so the initial state corresponds classically to a distribution concentrated on the v axis in state space r,v, with velocity (momentum) width Π. Scaling of (3.9) enables any r_0 to be transformed to $r_0=1$.

We will compare the classical and quantum trajectories. We showed [1] that the classical Newtonian trajectories $r(t)$ are determined by

$$r(t)^3\partial_{tt}r(t)=t^2, r(0)=1,\ \partial_t r(0)=v_0\,. \tag{3.14}$$

This represents a family of trajectories, parameterised by v_0. The quantum radial velocity at the spacetime point r,t is (cf (3.11))

$$u(r,t)=\hbar\partial_r\arg R(r,t)=\hbar\,\mathrm{Im}\left(\frac{\partial_r R(r,t)}{R(r,t)}\right), \tag{3.15}$$

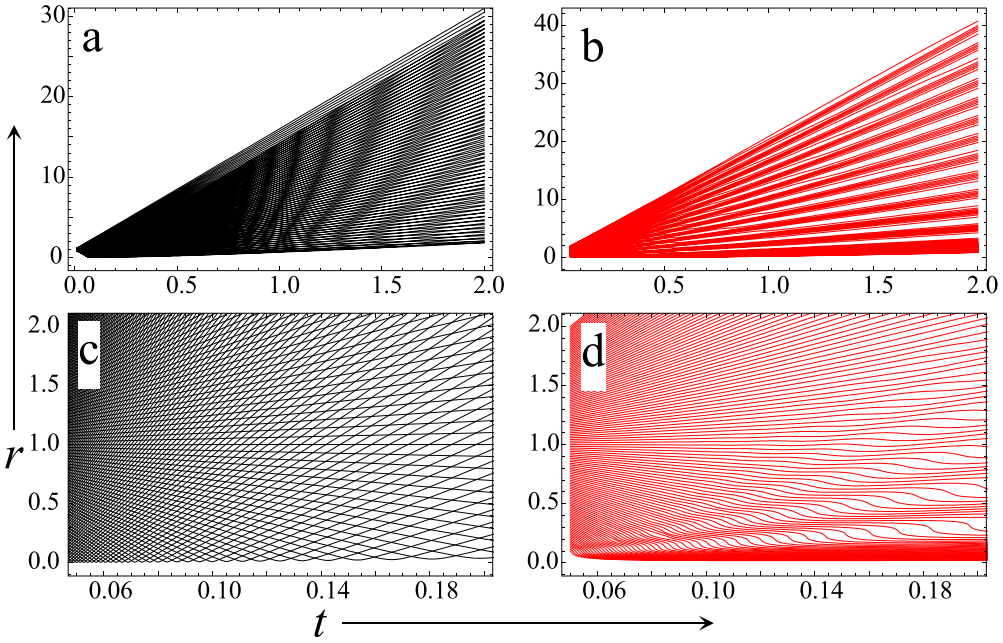

Figure 1. (a), (c): Classical trajectories; (b), (d): quantum trajectories, for $\hbar = \frac{1}{2}, \Pi = 40$; (c), (d) are magnifications of (a), (b).

where $R(r,t)$ is determined by (3.9) and the first of (3.13). Then the quantum trajectories $r(t)$ are the solutions of

$$d_t r(t) = u(r,t)\,,\; r(t_0) = r_0,\; (0 < t_0 \ll 1) \tag{3.16}$$

for different values of r_0. (The choice of small but nonzero t_0 reflects the very rapid spread of the wave away from $r = 1$; the results are not sensitive to t_0.)

Figure 1 illustrates the quantum and classical evolutions. Figure 1(a) shows classical paths, each calculated from (3.14) for a given value of the parameter v_0. Through each spacetime point in the wedge-shaped region in figure 1(a), bounded below by a caustic and above by a cutoff in v_0, two classical paths cross. These crossings give rise to the Moiré pattern, whose details depend on the choice of v_0 values; we chose $-15 \leqslant v_0 \leqslant 15$ with values separated by ¼. The crossings are clearly visible in the magnification in figure 1(c).

The quantum trajectories are entirely different: as described earlier, they do not cross. As figure 1(b) shows, they gather into bunches as t increases, reflecting the quantum oscillations of $R(r,t)$. The magnification (figure 1(d)) shows that the bunching is associated with undulations of the quantum trajectories (Newton's eels).

Appendix 3 describes two numerical checks of these calculations.

3.3. *Dynamics in the x,y plane*

Again invoking separability, we now reinstate θ and look at classical and quantum trajectories in the coordinate plane $\boldsymbol{r} = \{x,y\} = r\{\cos\theta, \sin\theta\}$, corresponding to the r trajectories in figure 1.

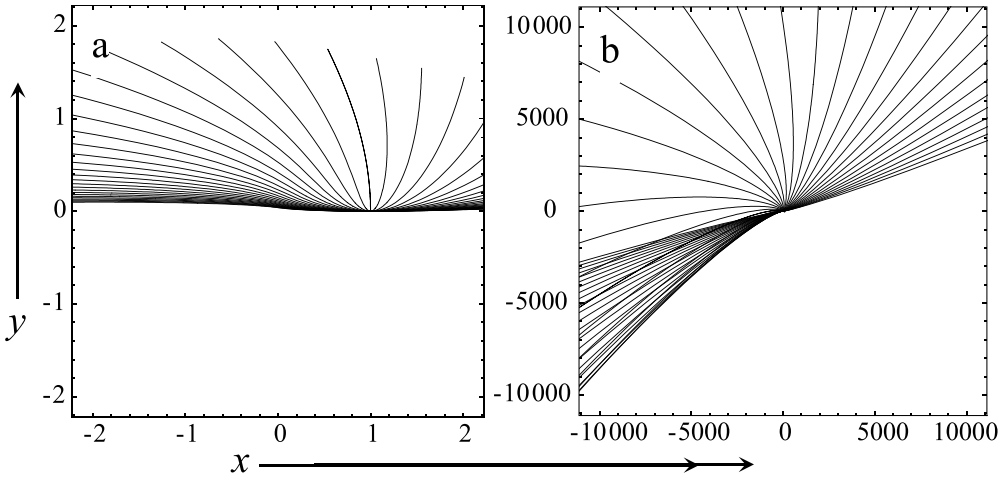

Figure 2. Family of classical trajectories in $\{x, y\}$ space for $0 \leqslant t \leqslant 2$, over (a) a smaller range, (b) a much larger range.

For the classical trajectories, we choose the family parameterised by v_0 as in (3.14) with $r_0 = 1$, $\partial_t r(0) = v_0$, and $\theta(0) = 0$, $\partial_t \theta(0) = 0$, i.e. $x(0) = 1$, $y(0) = 0$, $\partial_t x(0) = v_0$, $\partial_t y(0) = 0$. Thus, from the Hamiltonian (3.4) (conserved energy E), with angular momentum written as t,

$$E = \tfrac{1}{2}\left((\partial_t r)^2 + \tfrac{t^2}{r^2}\right) - \theta\,, \tag{3.17}$$

we fix $E = v_0^2/2$ and get

$$\theta(t) = \frac{1}{2}\left((\partial_t r(t))^2 - v_0^2 + \frac{t^2}{r(t)^2}\right). \tag{3.18}$$

Figure 2 shows this family in $\boldsymbol{r}$ space. Over the smaller range (figure 2(a)), they do not cross, but over much larger ranges (figure 2(b)) they do (as discussed in section 2). As we showed earlier [1], for vastly longer times, of order $t \sim \exp(4\pi^2 n^2) \sim (1.4 \times 10^{17})^{n^2}$, the trajectories will wind n times, with more crossings. The full family of classical trajectories corresponding to the quantum states we are describing are the patterns in figure 2, rotated, but it is clearer to show the unrotated family.

The quantum trajectories $\boldsymbol{r}(t)$ are generated by (2.10) with the quantum velocity $\boldsymbol{u}(\boldsymbol{r}, t)$ in (3.11). Figure 3 shows the intensity, with the instantaneous velocity field superimposed, at a particular time. The twirl of $\boldsymbol{u}$ near the origin reflects the underlying curl force, even for this mode with $m = 0$, for which Ψ is independent of θ.

Figure 4 shows the quantum trajectories corresponding to figure 1, on three different scales. On the largest scale (figure 4(a)), the undulations (Newton's eels) are not discernable. Zooming in (figure 4(b)), the undulations can be glimpsed for positive θ; and the crossing phenomenon described earlier can be seen: more than one trajectory can wind and reach the same $\boldsymbol{r}$ at different times, when $\boldsymbol{u}$ is different. Zooming further (figure 4(c)), Newton's eels are clearer; they form a hierarchy, with finer-scale undulations closer to the positive x axis.

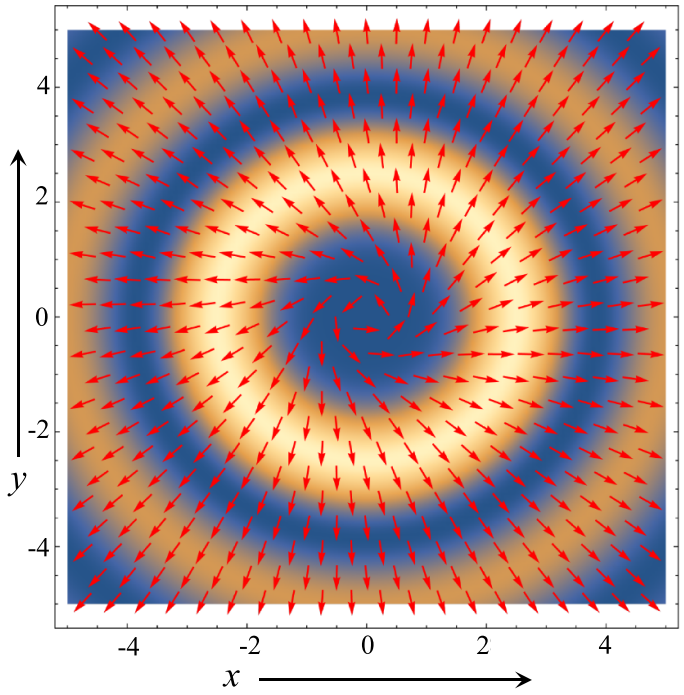

Figure 3. Intensity $|R(r,t)|^2$ and quantum velocity field $\boldsymbol{u}(r,t)$, for $t=2$, $\hbar=\frac{1}{2}$.

3.4. More general states

The initial state (3.13), concentrated near $r=r_0$, generates only one of the infinitely many solutions of the radial equation (3.9). Another interesting class of solutions is the set of instantaneous eigenstates of the operator in (3.9). These satisfy

$$-\frac{\hbar^2}{2r}\partial_r\left(r\partial_r R_k(r,t)\right)+\frac{t^2}{2r^2}R_k(r,t)=k^2R_k(r,t)\,, \tag{3.19}$$

with eigenvalue k^2, and are the Bessel functions

$$R_k(r,t)=J_{|t|/\hbar}\left(\sqrt{2}\tfrac{kr}{\hbar}\right), \tag{3.20}$$

possessing the unusual feature that the order increases linearly with time. These instantaneous eigenstates (which are not square-integrable, concordant with the unbound nature of the corresponding classical curl force dynamics [1]), are the building-blocks of the adiabatic approximation to the time-dependent solutions of (3.9).

4. Quantum curl force with velocity streamlines on cylinders

In this section, we will illustrate several features of quantum curl dynamics by contriving a specified steady three-dimensional velocity field with nonzero vorticity, and 'reverse-engineering' to determine the curl force that would generate it.

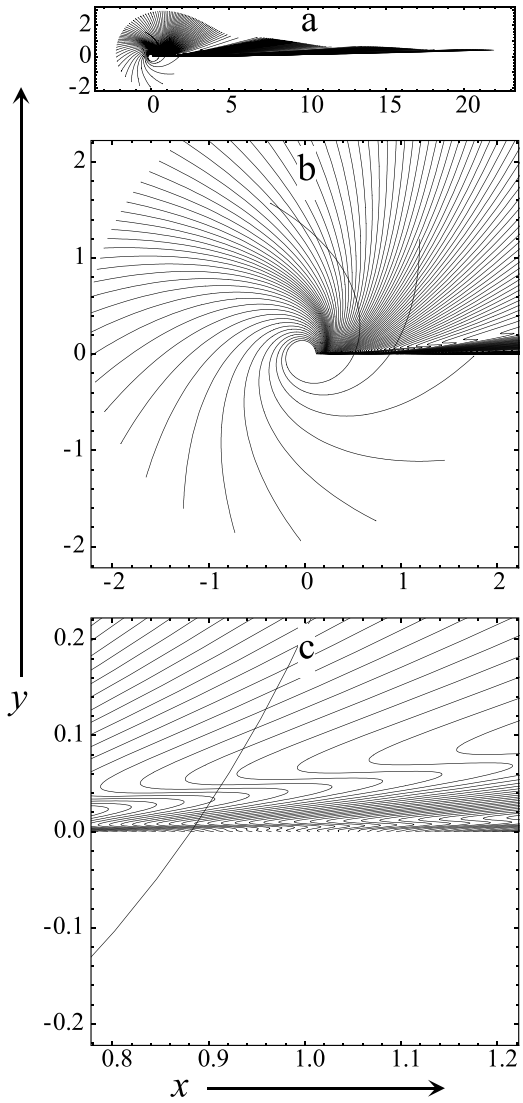

Figure 4. Quantum trajectories $\boldsymbol{r}(t)$ for $0 \geqslant t \geqslant 2$, $\hbar = 1/2$, illustrated on three different scales.

The field is

$$\boldsymbol{u} = \{1, -\varepsilon z\xi(x), \varepsilon y\xi(x)\}. \tag{4.1}$$

The parameter ε can be regarded as a perturbation, switching on the vorticity. Figure 5(a) illustrates one of the streamlines for the case

$$\xi(x) = \cos x, \varepsilon = 1. \tag{4.2}$$

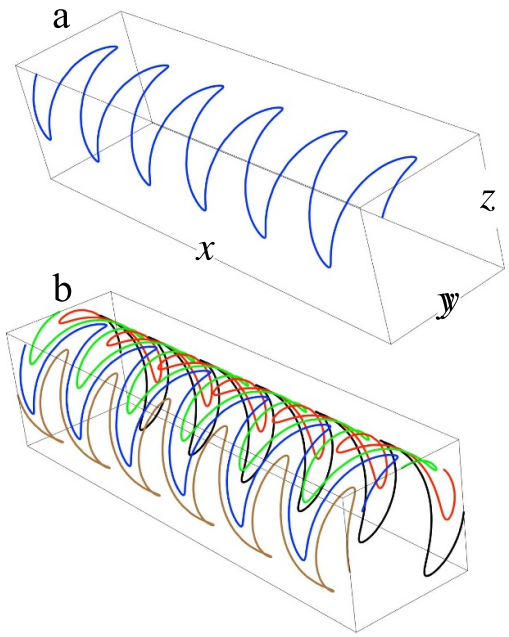

Figure 5. Streamlines of the field (4.1) and (4.2).

The streamlines oscillate on cylinders centred on the x axis, and the complete field of streamlines consists of copies, translated along x and rotated and expanded about the x axis. Figure 5(b) shows a few rotated streamlines.

The vorticity is non-zero for finite ε:

$$\boldsymbol{\omega} = \varepsilon\left\{2\xi\,(x)\,, -y\xi\,'(x)\,, -z\xi\,'(x)\right\}. \tag{4.3}$$

The field is not Beltrami:

$$\boldsymbol{u}\times\boldsymbol{\omega} = \varepsilon\left\{-\frac{1}{2}\varepsilon\left(y^2+z^2\right)\left(\xi\,(x)^2\right)',\, 2\varepsilon y\xi\,(x)^2 + z\xi\,'(x)\,,\, 2\varepsilon z\xi\,(x)^2 - y\xi\,'(x)\right\}. \tag{4.4}$$

In addition, the helicity field is nonzero:

$$\boldsymbol{u}\cdot\boldsymbol{\omega} = 2\varepsilon\xi\,(x). \tag{4.5}$$

A simple argument shows that this implies that $\boldsymbol{u}$ cannot rescaled to make $\boldsymbol{F}$ curl-free; such 'decurling' would lead to a velocity field with the same pattern of trajectories, differently traversed.

The particular field $\boldsymbol{u}$ in (4.1) is divergenceless:

$$\nabla\cdot\boldsymbol{u} = 0, \tag{4.6}$$

and so describes an incompressible flow. This is helpful in calculating the density ρ because the continuity equation (2.4) simplifies to

$$(\nabla\rho)\cdot\boldsymbol{u} = 0, \tag{4.7}$$

i.e. the gradient of the density is perpendicular to the flow. The calculation of densities compatible with velocity fields that are not incompressible is described in appendix 4. For the field (4.1) and (4.7) is satisfied by any density of the form

$$\rho = f\left(y^2 + z^2\right). \tag{4.8}$$

A convenient choice is

$$\rho = \exp\left(-\left(y^2 + z^2\right)\right), \tag{4.9}$$

representing a localised quantum beam driven by a curl force centred on the x axis.

The corresponding quantum potential is

$$V_Q = -\frac{\nabla^2\sqrt{\rho}}{2\sqrt{\rho}} = 1 - \frac{1}{2}\left(y^2 + z^2\right). \tag{4.10}$$

This generates a quantum force repulsive away from the x axis, which might seem puzzling. But note that, in the 'reverse-engineered' total external force (2.8), ∇V_Q occurs with a $+$ sign, attracting the quantum state near the x axis. (A helpful non-curl, i.e. potential force, example is the ground state of the 1D quantum simple harmonic oscillator. The wavefunction is real, so the velocity u is zero: the Madelung particles are stationary, so the quantum potential must be repulsive in order to cancel the attractive external potential.) A similar example, involving a linear potential, has also been interpreted in terms of the force from the quantum potential [35].)

The external force (2.8), that would generate particles moving along the streamlines of (4.1), is

$$\boldsymbol{F} = \varepsilon\left\{0, -\varepsilon y\xi(x)^2 - z\xi'(x) - y, -\varepsilon z\xi(x)^2 + y\xi'(x) - z\right\}, \tag{4.11}$$

correctly attracting the waves. And it is a curl force:

$$\nabla\times\boldsymbol{F} = \varepsilon\left\{2\xi'(x), 2\varepsilon z\left(\xi(x)^2\right)' - y\xi''(x), -2\varepsilon y\left(\xi(x)^2\right)' - z\xi''(x)\right\}. \tag{4.12}$$

Finally, the explicit form of the streamlines, solving

$$\partial_t \boldsymbol{r} = \boldsymbol{u}, \tag{4.13}$$

for the field (4.1) and the special case (4.2), is (using $x = t$ because $u_x = 1$), is

$$\boldsymbol{r} = \{x, c\cos(\gamma + \sin x), c\sin(\gamma + \sin x)\}, \tag{4.14}$$

where the amplitude c and phase γ are real.

The contrived velocity field (4.1) lacks the 'Newton's eel' undulations characteristic of Madelung streamlines, described in section 2 and illustrated in section 3; this demonstrates that there are quantum curl forces without these undulations.

5. Concluding remarks

The Madelung picture of quantum mechanics does not explicitly refer to a Schrödinger equation or a wavefunction. It has been argued [36] that in a counterfactual history, in which the wave equation had been discovered later, the Madelung representation (with the Bohmian interpretation) might be today's default picture. But of course there is a wave underlying the Madelung picture; its presence is betrayed by the singlevaluedness condition (2.6).

In our proposed generalisation to quantum curl forces, by adding the quantum potential to classical curl dynamics by analogy with the Madelung procedure for potential forces, there is in general no underlying singlevalued wavefunction. (The exceptional case studied in section 3 does involve a wavefunction, but before the gauge transformation it is not singlevalued in the plane.) In our exploration of this generalisation, we gave examples where it was not necessary to solve the nonlinearly coupled continuity and velocity equations (2.4) and (2.8) for a general curl force. Instead, in section 3 we were able to adapt standard quantum techniques to the unusual situation where the curl of the force was concentrated at a point, interpreting this as an unfamiliar time-dependent Aharonov–Bohm system. And in section 4 we specified the velocity field and by reverse-engineering determined the curl force that would generate it. The general case, for which these strategies are unavailable, seems difficult; it deserves further study.

A possible experimental implication of the quantum generalisation involves the forces exerted by light waves on small dielectric polarisable particles with complex polarisability α. Classically, these forces are of two kinds [37, 38]. There is the gradient force employed for trapping the particles; this is proportional to $\mathrm{Re}\alpha$. And there is a curl force (in optical terminology it is the 'scattering force'), proportional to $\mathrm{Im}\alpha$. As discussed elsewhere [6], there is no contradiction in the fact that curl force dynamics is nondissipative even though $\mathrm{Im}\alpha$ represents absorption by the particle.

For a monochromatic electric field represented by a complex position-dependent function $\boldsymbol{E}$, this curl force is proportional to

$$\mathrm{Im}\alpha\ \mathrm{Im}\left[\boldsymbol{E}^*\cdot(\nabla)\boldsymbol{E}\right], \tag{5.1}$$

so its curl is proportional to

$$\mathrm{Im}\alpha\ \mathrm{Im}\left[\nabla\boldsymbol{E}^*\cdot\times\nabla\boldsymbol{E}\right] \tag{5.2}$$

where the scalar product $\cdot$ links $\boldsymbol{E}^*$ and $\boldsymbol{E}$ and the vector product $\times$ links ∇ and ∇. (We note that (5.1) and (5.2) have the same forms as the geometric phase one-form and two-form respectively [39, 40].)

Quantum curl dynamics would correspond not to a single orbit of the polarisable particle but to a family of trajectories (without a curl force, this would correspond to a wavepacket). The family would depend on the initial conditions. Where the particles are detected would depend on which trajectory in the family is selected randomly.

Data availability statement

All data that support the findings of this study are included within the article (and any supplementary files).

Acknowledgments

We thank Professor John Hannay, Professor Cesare Tronci, and two referees for helpful comments. M V B's research is supported by the Leverhulme Trust. M V B thanks the Indian Institute of Technology, Kharagpur and the Bhabha Atomic Research Centre, Mumbai, for hospitality during this research. P S's research is supported by SERB, DST India under MATRICS Grant MTR/2019/000183.

Appendix A Anisotropic kinetic energy

It suffices to see how the Madelung quantum procedure, and its curl force extension, work, with slight modification, for the simplest anisotropic Hamiltonian: steady states of a 2D Hamiltonian in free space, with coordinates $\boldsymbol{r} = \{x, y\}$ and momenta $\boldsymbol{p} = \{p_x, p_y\}$. The Hamiltonian is

$$H = \frac{1}{2}\left(ap_x^2 + 2bp_xp_y + cp_y^2\right) = \frac{1}{2}\left(p_xp_y\right)M\begin{pmatrix} p_x \\ p_y \end{pmatrix}, \text{ where } M = \begin{pmatrix} a & b \\ b & c \end{pmatrix}. \tag{A1.1}$$

(We studied this classically in [41].) The Schrödinger equation (which could for example also describe optics in a uniform anisotropic medium), is conveniently written as

$$-\frac{\left(a\partial_{xx} + 2b\partial_{xy} + c\partial_{yy}\right)\psi}{2\psi} = E. \tag{A1.2}$$

The solution can be written in the polar form (2.1). For this anisotropic case, there are two distinct velocity fields: the phase velocity $\boldsymbol{u}$, which in this case is the canonical momentum

$$\boldsymbol{u} = \boldsymbol{p} = \nabla\chi, \tag{A1.3}$$

and the group velocity $\boldsymbol{v}$, which is the kinetic momentum—the physical velocity of particles in the flow field $\boldsymbol{u}$:

$$\boldsymbol{v} = \nabla_{\boldsymbol{p}}H = M\boldsymbol{u} = \{au_x + bu_y, u_x + cu_y\}. \tag{A1.4}$$

The desired Newtonian acceleration involves the kinetic (i.e. physical) $\boldsymbol{v}$, not the canonical $\boldsymbol{u}$:

$$d_tv = (\boldsymbol{v}\cdot\nabla)\,v. \tag{A1.5}$$

Substituting (2.1) into (A1.2) and evaluating the l.h.s. leads to an expression with a real part and an imaginary part. The imaginary part must be zero, leading to the continuity equation

$$\nabla\cdot(\rho\boldsymbol{v}) = 0, \tag{A1.6}$$

also involving $\boldsymbol{v}$ rather than the canonical $\boldsymbol{u}$.

The real part of (A1.2) leads (after some calculation) to

$$\frac{1}{2}\boldsymbol{u}\cdot\boldsymbol{v}+V_Q=E, \tag{A1.7}$$

in which the natural anisotropic Madelung quantum potential is

$$V_Q=-\frac{1}{2\sqrt{\rho}}\left(a\partial_{xx}+2b\partial_{xy}+c\partial_{yy}\right)\sqrt{\rho}\,. \tag{A1.8}$$

The r.h.s. of (A1.7) (energy) is constant, so the derivatives of the l.h.s with respect to x and y are zero.

A crucial step depends on the identity

$$\left(\boldsymbol{v}\cdot\nabla\right)v=M\nabla\left(\frac{1}{2}\boldsymbol{u}\cdot\boldsymbol{v}\right)=\begin{pmatrix} a\partial_x+b\partial_y \\ b\partial_x+c\partial_y \end{pmatrix}\left(\frac{1}{2}\boldsymbol{u}\cdot\boldsymbol{v}\right), \tag{A1.9}$$

whose proof depends on the irrotationality of $\boldsymbol{u}$ (cf (A1.3)). It leads to the main result, that the Madelung force (acceleration) of particles moving along the streamlines of $\boldsymbol{v}$ is

$$d_t\boldsymbol{v}=\boldsymbol{F}=-M\nabla V_Q. \tag{A1.10}$$

Explicitly,

$$\begin{pmatrix} d_tv_x \\ d_tv_y \end{pmatrix}=\frac{1}{2\sqrt{\rho}}\begin{pmatrix} a^2\partial_{xxx}++3ab\partial_{xxy}+\left(2b^2+ac\right)\partial_{xyy}+bc\partial_{yyy} \\ ab\partial_{xxx}+\left(2b^2+ac\right)\partial_{xxy}+3bc\partial_{xyy}+c^2\partial_{yyy} \end{pmatrix}\sqrt{\rho}\,. \tag{A1.11}$$

This result gives the Madelung trajectories for general quantum states governed by an anisotropic Hamiltonian. The quantum curl force version would correspond simply to adding a curl force to $\boldsymbol{F}$ in (A1.10).

Appendix B Two checks on calculations in section 3

The first check is a comparison of the solution of the radial equation (3.9) with its semiclassical approximation. For each r,t, the semiclassical contributions are found by evolving points with initial radial velocity v_0 on the line $r=1$, for time t, as a curve in the r,v, plane. Figure 6 shows the curve. The explanation of the hairpin shape is that points on the initial curve with $v_0>0$ move towards increasing r, and for points with $v_0<0$ r initially decreases before turning and then increasing (i.e. $v\left(t\right)$ is initially negative, then positive).

For each position r and time t, standard semiclassical theory [42, 43] indicates that there are interfering contributions from the two branches $v_0=v_{0\pm}\left(r,t\right)$, which are the solutions of

$$r\left(t,v_{0\pm}\right)=r. \tag{A2.1}$$

The intensity of each contribution is $1/\left|\partial_{v_0}r\left(t,v_{0\pm}\right)\right|$ weighted by the modulus of the initial momentum distribution in (3.13), and its phase $\gamma_\pm$ is the time integral of the Lagrangian (kinetic-potential energy, cf (3.9)), in units of $\hbar$:

$$\gamma_\pm\left(r,t\right)=\frac{1}{2\hbar}\int_0^t\mathrm{d}\tau\left(\left(\partial_\tau r\left(\tau,v_{0\pm}\right)\right)^2-\frac{\tau^2}{r\left(\tau,v_{0\pm}\right)^2}\right)\,. \tag{A2.2}$$

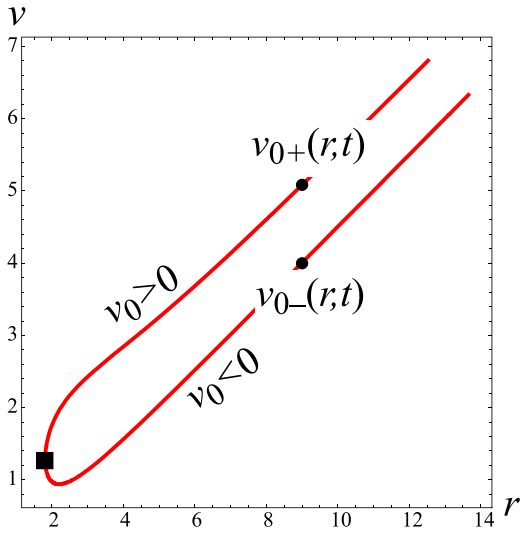

Figure 6. Phase space curve at $t = 2$, evolved from $r = 1$ at $t = 0$ for different values of initial radial velocity v_0; the branches meet at the caustic singularity (black square at $r \approx 1.811$).

Thus the semiclassical intensity is

$$I_{\rm sc}(r,t) = \frac{K}{r}\left|\frac{\exp\left(i\gamma_-(r,t) - \frac{v_{0-}^2}{2\Pi^2}\right)}{|\partial_{v_0} r_-(t,v_0)|^{\frac{1}{2}}} + i\frac{\exp\left(i\gamma_+(r,t) - \frac{v_{0+}^2}{2\Pi^2}\right)}{|\partial_{v_0} r_+(t,v_0)|^{\frac{1}{2}}}\right|^2, \tag{A2.3}$$

in which the factor i is the Stokes multiplier [43] between the contributions, and the factor $1/r$ arises from the polar coordinates.

Figure 7 illustrates the accuracy of the approximation. As always, the semiclassical approximation fails at the caustic singularity where the branches in figure 6 meet. This is easily fixed by the uniform approximation [44] in terms of the Airy function [45, 46]—now standard (section 36.12 in [47]), so it is not necessary to give details.

The second check is the continuity equation (2.4) associated with the one-dimensional r dynamics (3.9) and (3.15), namely

$$\frac{1}{r}\partial_r\left[r|R(r,t)|^2 u(r,t)\right] = -\partial_t|R(r,t)|^2. \tag{A2.4}$$

Figure 8 shows the two members of this equation as a function of r for fixed t, showing comfortable agreement.

Appendix C Wrapped and unwrapped angles

This refers to section 3 and the potential (3.3), in which the domain of θ is the full line $-\infty < \theta < \infty$, i.e. including windings, not the plane angle $0 \leqslant \theta < 2\pi$. Solutions of the Schrödinger equation (3.5) are singlevalued on the helicoid $-\infty < \theta < \infty$, $0 < r < \infty$, and solutions of the gauge-transformed Schrödinger equation (3.7) are smooth and periodic on the punctured plane

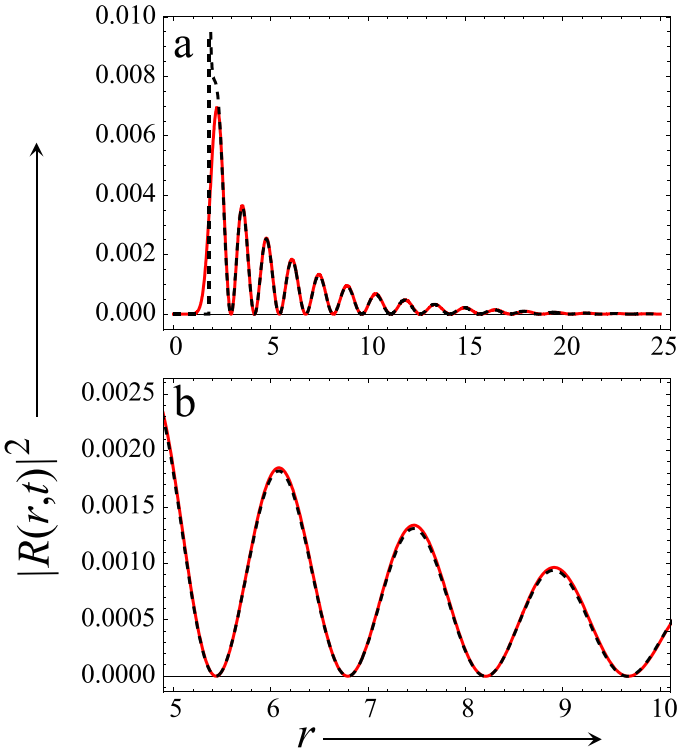

Figure 7. Comparison of the exact wave intensity $|R(r,t)|^2$ (solution of (3.9)) (red curve) with the semiclassical approximation (A2.3) (dashed black curve), for $t = 2$, $\hbar = \frac{1}{4}$, $\Pi = 40$; (a) shows the caustic singularity of the approximation, at $r = 1.811$; (b) magnification of (a).

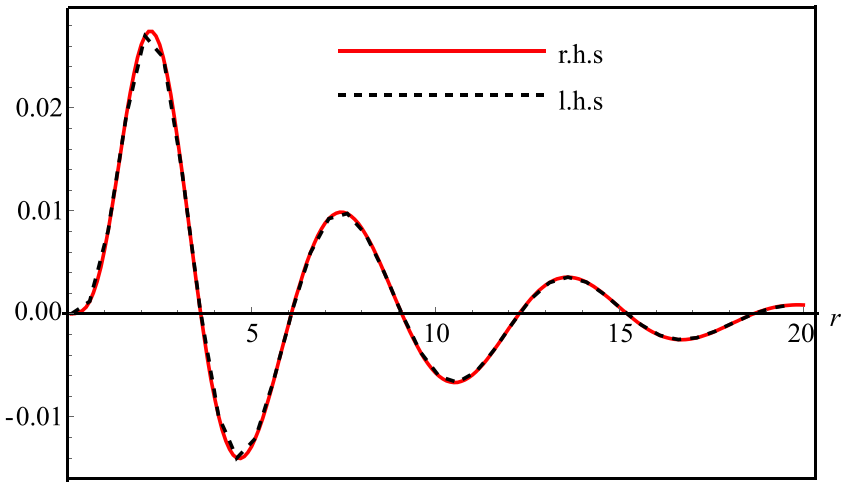

Figure 8. The two members of the continuity equation (A2.4), for $t = 2, \hbar = 1$.

$0 \leqslant \theta < 2\pi\,, 0 < r < \infty$. Connecting the two interpretations of the angle is the Poisson sum formula [47, 48]. Any periodic function can be expressed as a superposition of the windings of an unwrapped (i.e. not periodic) function:

$$\begin{aligned}\psi_{\,\text{periodic}}\,(\theta) &= \sum_{m-\infty}^{\infty} c\,(m)\exp\,(im\theta) \\ &= \sum_{n-\infty}^{\infty}\int_{-\infty}^{\infty} \mathrm{d}\mu c\,(\mu)\exp\,(i\mu\,(\theta+2m\pi\,)) \\ &= \sum_{n=-\infty}^{\infty} \psi_{\,\text{unwrapped}}\,(\theta+2n\pi\,)\,, \end{aligned} \tag{A3.1}$$

where

$$\psi_{\,\text{unwrapped}}\,(\theta) = \int_{-\infty}^{\infty} \mathrm{d}\mu c\,(\mu)\exp\,(i\mu\theta) \tag{A3.2}$$

and $c\,(\mu)$ is any reasonable interpolation of $c\,(m)$.

In physics, Poisson summation describes a general phenomenon: representing a sum over discrete eigenvalues as a sum over topologies. In the present case, the eigenvalues are angular momenta and the topologies are windings. Related examples of this association are the 'many-whirls' representation of the Aharonov–Bohm wavefunction [49, 50] and potential scattering by spheres [43, 51, 52]. In waveguides [53], the eigenvalues are modes, and the topologies are bouncings of rays at the walls. In electron microscopy of crystals [54], the eigenvalues denote Bloch waves and the topologies are undulations of classical paths. In the quantum mechanics of classically integrable systems [55], the eigenvalues are energies and the topologies are classical periodic orbits. In the optical Talbot effect [56, 57], the eigenvalues label diffracted beams and the topologies are image repetitions.

Appendix D Determining ρ from $\boldsymbol{u}$ for steady flows

For steady flows, the continuity equation (2.4) is

$$\nabla\cdot(\rho\boldsymbol{u}) = \boldsymbol{u}\cdot\nabla\rho + \rho\nabla\cdot\boldsymbol{u} = 0\,. \tag{A4.1}$$

For divergenceless flows, ρ can be any function constant along streamlines of $\boldsymbol{u}$, as in the example of section 4. The more interesting case is $\nabla\cdot\boldsymbol{u} \neq 0$. Then (A4.1) describes the variation of ρ along $\boldsymbol{u}$ but says nothing about the variation of ρ across the streamlines of $\boldsymbol{u}$. Any solution of (A4.1) can be multiplied by any solution ρ_0 of $\boldsymbol{u}\cdot\nabla\rho_0 = 0$. To get the contribution that depends on $\nabla\cdot\boldsymbol{u}$, we note that

$$\boldsymbol{u}\cdot\nabla = u\partial_s\,, \tag{A4.2}$$

where s is distance along a streamline. Therefore the solution of (A4.1), after writing it in the form

$$\boldsymbol{u}\cdot\nabla\log\rho = \boldsymbol{u}\partial_s\log\rho = -\nabla\cdot u, \tag{A4.3}$$

is

$$\rho = \rho_0 \exp\left(-\int_{r_0}^{r} ds \frac{\nabla\cdot\boldsymbol{u}}{u}\right) = \rho_0 \exp\left(-\int_{\boldsymbol{r}_0}^{\boldsymbol{r}} d\boldsymbol{r}\cdot\boldsymbol{u}\frac{\nabla\cdot\boldsymbol{u}}{u^2}\right), \tag{A4.4}$$

in which the integration path is along the streamline containing the point $\boldsymbol{r}$.

Integration along the streamline is important, because the integral depends on the path if

$$\nabla\times\left(\boldsymbol{u}\frac{\nabla\cdot\boldsymbol{u}}{u^2}\right)\neq 0, \tag{A4.5}$$

which is usually the case. This has an important implication for flows $\boldsymbol{u}$ containing streamlines in the form of closed loops. Then ρ cannot be singlevalued: around the loop; ρ changes by the factor

$$\frac{\rho_{\text{final}}}{\rho_{\text{initial}}} = \left(-\oint \mathrm{d}\boldsymbol{r}\cdot\boldsymbol{u}\frac{\nabla\cdot\boldsymbol{u}}{u^2}\right) = \exp\left(-\iint \mathrm{d}\boldsymbol{S}\cdot\nabla\times\left(\boldsymbol{u}\tfrac{\nabla\cdot\boldsymbol{u}}{u^2}\right)\right) \tag{A4.6}$$

where the final integration is over any surface spanning the closed streamline.

Here are three 2D examples illustrating the formalism.

Example 1. Shear flow. This velocity field (which for general h possesses both divergence and curl), and the classical curl force that generates it (the quantum potential is not relevant here), are

$$\boldsymbol{u} = h(x,y)\boldsymbol{e}_x, \quad \boldsymbol{F} = (\boldsymbol{u}\cdot\nabla)u = \left\{\frac{1}{2}\partial_x\left(h^2\right),0\right\}, \tag{A4.7}$$

so

$$\boldsymbol{\omega} = -\partial_y h\boldsymbol{e}_z, \quad \nabla\times\boldsymbol{F} = -\left(\partial_x h\partial_y h - h\partial_{xy}h\right)\boldsymbol{e}_z\,. \tag{A4.8}$$

In (A4.4), the integration is along x and the integrand is

$$\frac{\nabla\cdot\boldsymbol{u}}{u} = \frac{\partial_x h}{h} = \partial_x \log h, \tag{A4.9}$$

so the density is (writing the arguments explicitly)

$$\rho(x,y) = \frac{\rho_0(y)}{h(x,y)}, \text{ i.e. } \rho\boldsymbol{u} = \{\rho_0(y),0\} \tag{A4.10}$$

whose divergence vanishes, so continuity is satisfied.

Example 2: Radial flow without rotation symmetry. This is (using polar coordinates)

$$\boldsymbol{u} = g(\theta)\{x,y\} = rg(\theta)\boldsymbol{e}_r. \tag{A4.11}$$

For general g this has both div and curl:

$$\nabla\cdot\boldsymbol{u} = 2g(\theta), \nabla\times\boldsymbol{u} = -g'(\theta)\boldsymbol{e}_z\,. \tag{A4.12}$$

It is generated by a classical curl force

$$\boldsymbol{F} = (\boldsymbol{u}\cdot\nabla)\boldsymbol{u} = r(g(\theta))^2\boldsymbol{e}_r \tag{A4.13}$$

in which

$$\nabla \times \boldsymbol{F} = -\left(g^2\right)' \boldsymbol{e}_z \,. \tag{A4.14}$$

In (A4.4), the integration is along r and the integrand is

$$\frac{\nabla \cdot \boldsymbol{u}}{u} = \frac{2}{r}, \tag{A4.15}$$

so the density is (again writing the arguments explicitly)

$$\rho\left(r,\theta\right) = \frac{\rho_0\left(\theta\right)}{r^2}, \text{ i.e } \rho\boldsymbol{u} = \frac{\rho_0\left(\theta\right) g\left(\theta\right)}{r^2}\left\{x,y\right\} = \frac{\rho_0\left(\theta\right) g\left(\theta\right)}{r}\boldsymbol{e}_r, \tag{A4.16}$$

whose divergence vanishes, so continuity is satisfied.

Example 3: The simplest nontrivial azimuthal curl force. This is

$$\boldsymbol{F} = \boldsymbol{e}_\theta = \partial_{tt}\boldsymbol{r} = \frac{1}{r}\left\{-y,x\right\} \tag{A4.17}$$

and

$$\nabla \times \boldsymbol{F} = \frac{\boldsymbol{e}_z}{r}. \tag{A4.18}$$

The dynamics is exactly solvable (it is the special case $\mu = 0$ in [1]): in polar coordinates,

$$r\left(t\right) = \frac{t^2}{3\sqrt{2}},\ \theta\left(t\right) = \sqrt{2}\log t\,. \tag{A4.19}$$

Differentiation leads naturally to a velocity field that is a function of position rather than t:

$$\boldsymbol{u} = 2^{1/4}\sqrt{\frac{r}{3}}\left\{\sqrt{2}\boldsymbol{e}_r + \boldsymbol{e}_\theta\right\} = \frac{2^{1/4}}{\sqrt{3r}}\left\{x\sqrt{2}-y, x+y\sqrt{2}\right\}. \tag{A4.20}$$

This has nonzero curl and divergence

$$\nabla \times \boldsymbol{u} = \boldsymbol{\omega} = \frac{\sqrt{3}}{2^{3/4}}\frac{\boldsymbol{e}_z}{\sqrt{r}}, \quad \nabla \cdot \boldsymbol{u} = \frac{\sqrt{3}}{2^{1/4}\sqrt{r}}\,. \tag{A4.21}$$

The unexpected feature of this example is that we can calculate the density ρ analytically, using (A4.1) and (A4.4), involving ρ_0 which is any function that is constant along streamlines. Such a function is

$$\rho_0 = \frac{\exp\left(\sqrt{2}\theta\right)}{r}\,. \tag{A4.22}$$

For the line integral in (A4.4), we use

$$d\boldsymbol{r}\cdot\boldsymbol{u}\frac{\nabla\cdot\boldsymbol{u}}{\boldsymbol{u}^2} = \boldsymbol{u}dt\cdot\boldsymbol{u}\frac{\nabla\cdot\boldsymbol{u}}{\boldsymbol{u}^2} = dt\nabla\cdot\boldsymbol{u} = \frac{3dt}{t}, \tag{A4.23}$$

giving the density

$$\rho = \frac{\rho_0}{r^{3/2}} \tag{A4.24}$$

where ρ_0 is any function of (A4.22). The simplest choice is (A4.22) itself, for which

$$\rho = \frac{\exp\left(\sqrt{2}\theta\right)}{r^{5/2}}. \tag{A4.25}$$

This density is not singlevalued, and indeed it cannot be made so by any choice of ρ_0 for which ρ is non-negative, because the integral involving $\nabla \cdot \boldsymbol{u}$ in (A4.4) accumulates in a circuit of the origin. It is interesting that although ρ is not singlevalued, the quantum potential derived from it is singlevalued for some choices of ρ_0 but not all. In particular, it is singlevalued for the choice (A4.25):

$$V_Q = \frac{-\nabla^2\sqrt{\rho}}{2\sqrt{\rho}} = -\frac{33}{32r^2}. \tag{A4.26}$$

With the dynamics (A4.17) and (A4.19), the $\boldsymbol{u}, \rho$ pair (A4.20) and (A4.26) describes two consistent classical fields. But when the quantum force is added to the azimuthal curl force (A4.17), the resulting trajectories are different and no longer correctly linked to the trajectories by continuity. Making them compatible seems a difficult nonlinear self-consistency problem. Of course, reverse-engineering the pair (A4.17) and (A4.19) to correctly include the force from the quantum potential can be achieved by replacing the 'external' force (A4.17) by

$$\boldsymbol{F} = \boldsymbol{e}_\theta + \nabla V_Q, \tag{A4.27}$$

but like all quantum curl reverse-engineerings this simply amounts to adding and subtracting ∇V_Q. It misses the essential features of quantum curl dynamics when the external force is a purely classical curl force, and $-\nabla V_Q$ is a kind of internal nonlocal essentially quantum force.

ORCID iDs

M V Berry https://orcid.org/0000-0001-7921-2468
Pragya Shukla https://orcid.org/0000-0001-5308-6520

References

[1] Berry M V and Shukla P 2012 Classical dynamics with curl forces, and motion driven by time-dependent flux *J. Phys. A: Math. Theor.* **45** 305201
[2] Berry M V and Shukla P 2016 Curl force dynamics: symmetries, chaos, and constants of motion *New. J. Phys.* **18** 063018
[3] Sugiyama Y, Langthjem M A and Ryu B-J 1999 Realistic follower forces *J. Sound Vib.* **225** 779–82
[4] Sugiyama Y, Ryu S-U and Langthjem M A 2002 Beck's column as the ugly duckling *J. Sound Vib.* **254** 407–10
[5] Elishakoff I 2005 Controversy associated with the so-called 'follower forces': critical overview *Appl. Math. Rev.* **58** 117–42
[6] Berry M V and Shukla P 2013 Physical curl forces: dipole dynamics near optical vortices *J. Phys. A* **46** 422001
[7] Madelung E 1927 Quantentheorie in hydrodynamische form *Z. Phys.* **40** 322–6
[8] de Broglie L and Brillouin L 1928 *Selected Papers on Wave Mechanics* (Blackie)
[9] Bohm D 1951 *Quantum Theory* (Prentice-Hall, Inc)
[10] Bohm D 1952 A suggested interpretation of the quantum theory in terms of 'Hidden' variables I *Phys. Rev.* **85** 166–79
[11] Takabayasi T 1952 On the formulation of quantum mechanics associated with classical picture *Prog. Theor. Phys.* **8** 143–82

[12] Takabayasi T 1953 Remarks on the formulation of quantum mechanics with classical pictures and on relation between linear scalar fields and hydrodynamical fields *Prog. Theor. Phys.* **9** 187–222
[13] Foskett M S and Tronci C 2022 Holonomy and vortex structures in quantum hydrodynamics *Hamiltonian Systems: Dynamics, Analysis, Applications* (*Mathematical Sciences Research Institute Publications*) ed A Fathi, P J Morrison, T-M Seara and S Tabachnikov (Cambridge University Press) (arXiv:2003.08664)
[14] Loffredo M I and Morato L M 1993 On the creation of quantized vortex lines in rotating He II *Nuovo Cim.* **108B** 205–15
[15] Holland P 1993 *The Quantum Theory of Motion: An Account of the de Broglie Bohm Causal Interpretation of Quantum Mechanics* (University Press)
[16] Wallstrom T C 1994 Inequivalence between the Schrödinger equations and the Madelung hydrodynamic equations *Phys. Rev.* A **49** 1613–7
[17] Reddiger M 2017 The Madelung picture as a foundation of geometric quantum theory *Found. Phys.* **47** 1317–67
[18] Reddiger M and Poirier B 2023 Towards a mathematical theory of the Madelung equations: Takabayasi's quantization condition, quantum quasi-irrotationality, weak formulations, and the Wallstrom phenomenon *J. Phys. A: Math. Theor.* **56** 193001
[19] Heifetz E and Cohen E 2015 Toward a thermo-hydrodynamic like description of Schrödinger equation via the Madelung formulation and Fisher information *Found. Phys.* **45** 1514–25
[20] Heifetz E, Tsekov R, Cohen E and Nussinov Z 2016 On entropy production in the Madelung fluid and the role of Bohm's potential in classical diffusion *Found. Phys.* **46** 815–24
[21] Berry M V 2020 Superoscillations and the quantum potential *Eur. J. Phys.* **42** 015401
[22] Silva-Ortigoza G, Julián-Mácias I, Espinidola-Ramos E and Silva-Ortigoza R 2023 Exact and geometrical optics energy trajectories in Bessel beams via the quantum potential *J. Opt. Soc. Am.* B **40** 620–30
[23] Silva-Ortigoza G, Ortiz-Flores J, Sosa-Sánches C T and Silva-Ortigoza R 2023 The mechanical properties of the particle associated with the Lagerre-Gauss beams via the quantum potential point of view *J. Opt. Soc. Am.* B **40** 215–23
[24] Nye J F and Berry M V 1974 Dislocations in wave trains *Proc. R. Soc.* A **336** 165–90
[25] Riess J 1970 Nodal structure of Schroedinger wave functions and its physical significance *Ann. Phys.* **57** 301–21
[26] Riess J 1970 Nodal structure, nodal flux fields, and flux quantization in stationary quantum states *Phys. Rev.* D **2** 647–53
[27] Rubinsztein-Dunlop H *et al* 2017 Roadmap on structured light *J. Opt.* **18** 013001
[28] Nye J F 1999 *Natural Focusing and Fine Structure of Light: Caustics and Wave Dislocations* (Institute of Physics Publishing)
[29] Dirac P A M 1931 Quantised singularities in the electromagnetic field *Proc. R. Soc.* A **133** 60–72
[30] Holm D D 2008 *Geometric Mechanics; Part I: Dynamics and Symmetry; Part II: Translating and Rolling* (Imperial College Press)
[31] Newton I 1952 *1730.Opticks: Or a Treatise of the Reflections, Inflections and Colours of Light* 4th corrected edn (Dover)
[32] Berry M V 2002 Exuberant interference: rainbows, tides, edges, (de)coherence *Phil. Trans. R. Soc.* A **360** 1023–37
[33] Berry M V 1997 'Slippery as an eel', review of 'The fire within the eye', by David Park *Phys. World* **10** 41–42
[34] Berry M V 2017 In praise of Whig history, published as approaches to studying our history *Phys. Today* **70** 11–12
[35] Heifetz E and Cohen E 2020 Madelung transformation of the quantum bouncer problem *EPL* **130** 10002
[36] Cushing J T 1994 *Quantum Mechanics: Historical Contingency and the Copenhagen Hegemony* (University of Chicago Press)
[37] Ashkin A and Gordon J P 1983 Stability of radiation-pressure particle traps: an optical Earnshaw theorem *Opt. Lett.* **8** 511–3
[38] Gómez-Medina R, Nieto-Vesperinas M and Sáenz J J 2011 Nonconservative electric and magnetic optical forces on submicron dielectric particles *Phys. Rev.* A **83** 033825
[39] Berry M V 1984 Quantal phase factors accompanying adiabatic changes *Proc. R. Soc.* A **392** 45–57
[40] Berry M V and Shukla P 2019 Geometry of 3D monochromatic light: local wavevectors, phases, curl forces and superoscillations *J. Opt.* **21** 064002

[41] Berry M V and Shukla P 2015 Hamiltonian curl forces *Proc. R. Soc.* A **471** 20150002
[42] Van Vleck J H 1928 The correspondence principle in the statisticaql interpretation of quantum mechanics *Proc. Natl Acad. Sci. USA* **14** 178–88
[43] Berry M V and Mount K E 1972 Semiclassical approximations in wave mechanics *Reps. Prog. Phys.* **35** 315–97
[44] Temme N M 2015. *Asymptotic Methods for Integrals* (World Scientific)
[45] Vallée O and Soares M 2010 *Airy Functions and Applications to Physics* 2nd edn (Imperial College Press)
[46] Airy G B 1838 On the intensity of light in the neighbourhood of a caustic *Trans. Cambridge Philos. Soc.* **6** 379–402
[47] DLMF 2010 *NIST Handbook of Mathematical Functions* (University Press) (available at http:////dlmf.nist.gov)
[48] Lighthill M J 1958 *Introduction to Fourier Analysis and Generalized Functions* (University Press)
[49] Berry M V 1980 Exact Aharonov-Bohm wave function obtained by applying Dirac's magnetic phase factor *Eur. J. Phys.* **1** 240–4
[50] Berry M V 2010 Asymptotics of the many-whirls representation for Aharonov-Bohm scattering *J. Phys. A: Math. Theor.* **43** 354002
[51] Berry M V 1966 Uniform approximation for potential scattering involving a rainbow *Proc. Phys. Soc.* **89** 479–90
[52] Nussenzveig H M 1992 *Diffraction Effects in Semiclassical Scattering* (Cambridge University Press)
[53] Pekeris C L 1950 Ray theory vs normal mode theory in wave propagation problems *Proc. Symp. Appl. Math.* **2** 71–75
[54] Berry M V 1971 Diffraction in crystals at high energies *J. Phys. C: Solid State Phys.* **4** 697–722
[55] Berry M V and Tabor M 1976 Closed orbits and the regular bound spectrum *Proc. R. Soc.* A **349** 101–23
[56] Berry M V and Klein S 1996 Integer, fractional and fractal Talbot effects *J. Mod. Opt.* **43** 2139–64
[57] Berry M V and Bodenschatz E 1999 Caustics, multiply-reconstructed by Talbot interference *J. Mod. Opt.* **46** 349–65